

Supporting Information

Methyl-Functionalized Anionic MOFs for Charge- and Shape- Selective Adsorption of Dyes in Water Remediation

Qiuxia Wu,^{a#} Yuyang Liu,^{a#} Ruiqi Zhu,^a Lin Zhang,^{*a} Dian Zhao,^a Yabing He^{*a} and
Banglin Chen^{*ab}

^a Key Laboratory of the Ministry of Education for Advanced Catalysis Materials, College of Chemistry and Materials Science, Zhejiang Normal University, Jinhua 321004, China. E-mail: linzhang@zjnu.edu.cn; heyabing@zjnu.cn

^b Fujian Provincial Key Laboratory of Polymer Materials, College of Chemistry & Materials Science, Fujian Normal University, Fuzhou, 350007, P.R. China. E-mail: banglin.chen@fjnu.edu.cn

[#] These authors contributed equally to this work and should be considered co-first authors.

1. Experimental Section

Reagents and Chemicals.

All solvents and chemicals were purchased from commercial sources and used for synthesis without purification. To determine the purity of the samples, X-ray powder diffraction (PXRD) data of the samples were tested using a D8 Advance model X-ray powder diffractometer. The conditions were set to a sweep speed of $0.1^\circ/\text{s}$ at room temperature and a 2θ of $3\text{-}45^\circ$, and PXRD data were collected with Cu-K α rays ($\lambda = 1.5418 \text{ \AA}$). Fourier Transform Infrared (FTIR) data were obtained by Nicolet 5DX FTIR IR spectrometer in the wavelength range of $4000\text{-}400 \text{ cm}^{-1}$ and testing the samples by potassium bromide compression method. Thermogravimetric (TGA) curves were obtained by testing the samples and collecting data on a Netzsch STA F5 thermal analyzer under conditions of room temperature ramping to 1073 K at a rate of 10 K min^{-1} while maintaining a nitrogen atmosphere. Zeta potential was determined at room temperature using a Zetasizer Nano ZS 90 analyzer. UV-vis absorption spectra were tested using a UH5300 UV-visible spectrophotometer from Hitachi, Japan with a scanning speed of 400 nm/min .

Preparation of ZJU-64 and ZJU-64-Me.

ZJU-64 and ZJU-64-Me were synthesized based on the modification of the method reported in the literature.¹ Adenine (10 mg), [1,1':4',1''-biphenyl]-4,4''-dicarboxylic acid (H₂TP, 30 mg), zinc nitrate hexahydrate (100 mg) were sequentially added to a PTFE lined vessel followed by the addition of DMF (12 mL), water (1.5 mL) and nitric acid (60 μL) with a stainless-steel jacket. The reaction was carried out in an oven at $130 \text{ }^\circ\text{C}$ for 24 h. After the solution was cooled down to room temperature, it was washed several times with DMF and ethanol, respectively. The transparent crystals were extracted and filtered, and after the sample was dried, it was grinded to powder for subsequent tests.

The synthesis conditions of ZJU-64-Me were similar to those of ZJU-64 except that the second ligand was changed to 2',5'-dimethyl-[1,1':4',1''-biphenyl]-4,4''-dicarboxylic acid (H₂TP-C).

Preparation of ZJU-64-Me@SA membranes and SA membranes.

ZJU-64-Me with good crystal quality and sodium alginate were selected to make the membrane. Sodium alginate (50 mg), ZJU-64-Me (50 mg) were weighed in a 20 mL bottle and 2.5 mL of water was added. The mixed solution was stirred well, and 520 mg of the mixed solution was placed on glass sheet. Using a 750 nm spatula to push the mixed solution away at a constant speed, followed by placing it in a 1.5 wt % aqueous calcium chloride solution. After the membrane was formed, it was transferred to deionized water for a period of time to remove the free calcium ions. The SA membrane was prepared similarly to that of ZJU-64-Me@SA, except that the mass of the mixed solution was changed to 510 mg.

Dye adsorption and separation.

Powdery ZJU-64 and ZJU-64-Me: 10 mg of the grounded powder materials were homogeneously dispersed in 20 mL of organic dye solution, and the adsorption was allowed to stand at room temperature

for 30 min, and then 3 mL of the solution was sucked up with a filter, filtered in a cuvette, and the UV-visible absorption spectra of the supernatant were tested (300-800 nm).

ZJU-64-Me@SA membrane: 520 mg of the membrane was placed in an organic dye solution and left to adsorb for 1 h at room temperature, then the UV-visible absorption spectra (300-800 nm) of the solution were tested.

Kinetic adsorption test (MB for example): ZJU-64-Me (10 mg) or ZJU-64-Me@SA (520 mg) was added in a 50 mL centrifuge tube containing MB dye (10 ppm, 20 mL), the supernatant was taken at certain time intervals to test the absorbance of MB in the 300-800 nm band.

Isothermal adsorption test (MB as an example): ZJU-64-Me powder (10 mg) was added to a 50 mL centrifuge tube containing MB dye (20 mL) at different concentrations (5, 10, 20, 100, 120, 140, 160, 180, 200, 300, 400 ppm). ZJU-64-Me@SA (520 mg) was added to a 50 mL centrifuge tube containing MB dye (20 mL) at different concentrations (5, 50, 100, 150, 200, 300, 400, 600, 700, 800, 900, 1000, 1500, 2000 ppm). The adsorption isotherms of ZJU-64-Me powder and ZJU-64-Me@SA for MB were collected at room temperature. Five days of static adsorption. The UV-Vis absorption spectra (300-800 nm) of the solutions were tested.

Reusability.

In this work, the ZJU-64-Me powder samples after adsorption of MB were immersed in sodium hydroxide solution with PH = 11 for 3 min, and then soaked in ethanol for 12 h. Finally, the samples were washed thoroughly with deionized water and dried in an oven at 60 °C, and then repeated adsorption tests were carried out to observe the adsorption performance of the treated ZJU-64-Me on MB. A total of five repeated adsorption tests were performed.

The models for adsorption kinetics

To further explore the dynamic interactions between SA, ZJU-64-Me, ZJU-64-Me@SA, and dyes, we used a variety of kinetic models to fit the experimental data, including a pseudo-first-order model, a pseudo-second-order model, and an intra-particle diffusion model. The expressions for the kinetic models are as follows:

$$\ln(Q_e - Q_t) = \ln Q_e - k_1 t \quad (1)$$

$$\frac{t}{Q_t} = \frac{1}{Q_e^2} k_2^{-1} + \frac{t}{Q_e} \quad (2)$$

$$Q_t = k_i t^{0.5} + C \quad (3)$$

where Q_t (mg/g) denotes the amount of MB adsorbed at time (t), Q_e (mg/g) denotes the equilibrium adsorption amount, and t (min) denotes the adsorption time, k_1 (min^{-1}), k_2 ($\text{g mg}^{-1} \text{min}^{-1}$) and k_i ($\text{mg g}^{-1} \text{min}^{-0.5}$) denote the reaction rate constant.

The models for adsorption isotherm

To further investigate the adsorption isotherm of dye by SA, ZJU-64-Me and ZJU-64-Me@SA, Langmuir, Freundlich and Temkin models were used to fit the experimental data. The linear equations of these models are as follows

$$\frac{C_e}{Q_e} = \frac{1}{Q_m k_L} + \frac{C_e}{Q_m} \quad (4)$$

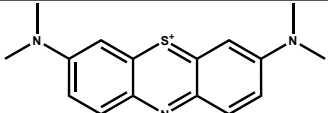
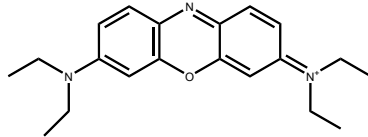
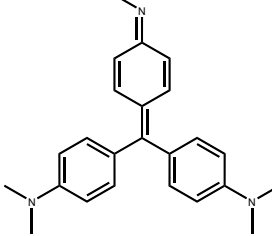
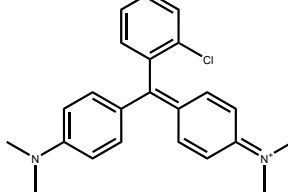
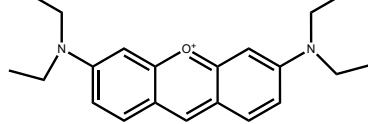
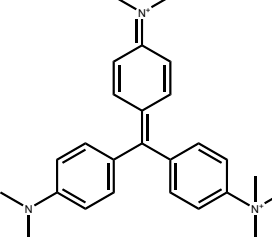
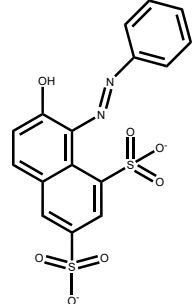
$$\ln Q_e = \ln k_F + \frac{1}{n} \ln C_e \quad (5)$$

$$Q_e = \frac{RT}{b_T} \ln C_e + \frac{RT}{b_T} \ln K_T \quad (6)$$

where C_e (mg/L) represents the dye concentrations at equilibrium, Q_e and Q_m (mg/g) represent the equilibrium and maximum adsorption amount of dye. K_L (L/mg) and K_F ($\text{mg}^{1-(1/n)} \text{L}^{1/n} \text{g}^{-1}$) represent the Langmuir and Freundlich adsorption constants, respectively. K_T (L/mg) and b_T (kJ mol^{-1}) is equilibrium binding constant and the Temkin isotherm constant, respectively. T (K) is temperature and R ($8.314 \times 10^{-3} \text{ kJ mol}^{-1} \text{ K}^{-1}$) is gas constant.

2. Supplementary Tables and Figures

Table S1. Physical-chemical properties of the selected dyes.

Dyes	Chemical structure	Size	M _r	change	λ _{max} (nm)
Methylene Blue (MB)		16.723×8.3 54×4.450	319.85	cationic	664
Basic Blue 3 (BB-3)		19.197×9.3 20×4.201	360.91	cationic	654
Methyl Violet (MV)		15.405×14. 312×5.810	393.96	cationic	582
Basic Blue 1 (BB-1)		15.340×11. 998×6.715	399.36	cationic	630
Pyronine B (PB)		14.293×10. 087×6.287	302.80	cationic	546
Malachite green (MG)		15.578×12. 336×6.447	364.92	cationic	616
Acid Orange G (AOG)		18.641×10. 879×4.885	452.37	anionic	476

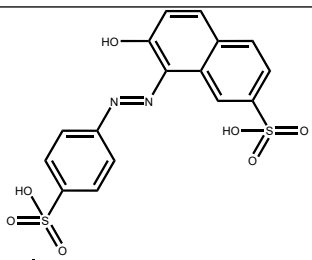
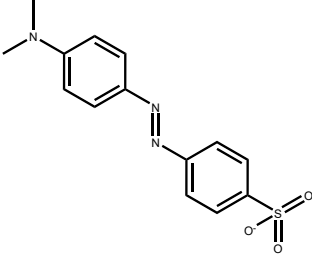
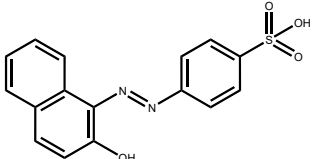
Sunset Yellow (SY)		21.740×11.498×6.600	452.36	anionic	480
Methyl Orange (MO)		17.602×7.490×6.429	327.33	anionic	476
Acid Orange 7(OI)		19.776×8.988×4.760	350.32	anionic	483

Table S2. Parameters related to kinetics of different MOF:SA ratios.

	1:2	3:2	2:1	5:2
--	-----	-----	-----	-----

Pseudo first-order	Q_e (mg·g ⁻¹)	6.826	5.085	6.525	4.755
	K_1 (min ⁻¹)	0.0289	0.0259	0.0196	0.0156
	R ²	0.9954	0.9836	0.9986	0.9946
Pseudo second-order	Q_e (mg·g ⁻¹)	7.897	5.9159	7.952	5.961
	K_1 (min ⁻¹)	0.0045	0.0054	0.0026	0.0026
	R ²	0.9793	0.9979	0.9893	0.9991

Table S3. Parameters related to kinetics of ZJU-64-Me and ZJU-64-Me.

	SA	ZJU-64-Me	ZJU-64-Me@SA
Pseudo first-order	Q_e (mg·g ⁻¹)	12.31	Q_e (mg·g ⁻¹) 20.33
	K_1 (min ⁻¹)	0.0245	K_1 (min ⁻¹) 0.0500
	R ²	0.9926	R ² 0.9870
Pseudo second-order	Q_e (mg·g ⁻¹)	14.18	Q_e (mg·g ⁻¹) 22.45
	K_2 (g·mg ⁻¹ ·min ⁻¹)	0.0021	K_2 (g·mg ⁻¹ ·min ⁻¹) 0.0033
	R ²	0.9979	R ² 0.9379

Table S4. Parameters related to internal diffusion modelling for SA, ZJU-64-Me and ZJU-64-Me@SA.

	SA			ZJU-64-Me			ZJU-64-Me@SA		
	K_d	C	R ²	K_d	C	R ²	K_d	C	R ²
Step 1	1.221	-0.1791	0.9961	3.901	-5.381	0.9981	0.8373	-0.8653	0.9977
Step 2	0.4980	5.660	0.9585	1.375	9.854	0.9441	0.3976	3.1436	0.9825
Step 3	0.1305	10.31	0.9853	0.0132	19.81	0.4595	0.1420	6.8296	0.9589

Table S5. Parameters related to the isothermal model for SA, ZJU-64-Me and ZJU-64-Me@SA.

	SA		ZJU-64-Me		ZJU-64-Me@SA	
	Q_m (mg·g ⁻¹)	995.9	Q_m (mg·g ⁻¹)	244.1	Q_m (mg·g ⁻¹)	766.4
Langmuir	K_l (L·mg ⁻¹)	0.0318	K_l (L·mg ⁻¹)	0.0529	K_l (L·mg ⁻¹)	0.0219
	R ²	0.9268	R ²	0.9801	R ²	0.9708
Freundlich	Q_m (mg·g ⁻¹)	134.2	Q_m (mg·g ⁻¹)	96.19	Q_m (mg·g ⁻¹)	119.7
	K_f (mg ^{1-1/n} ·L ^{1/n} ·g ⁻¹)	-0.3254	K_f (mg ^{1-1/n} ·L ^{1/n} ·g ⁻¹)	-0.1545	K_f (mg ^{1-1/n} ·L ^{1/n} ·g ⁻¹)	-0.2760
	R ²	0.7737	R ²	0.9559	R ²	0.8280
Temkin	A (L mg ⁻¹)	2.795	A (L mg ⁻¹)	4.887	A (L mg ⁻¹)	3.997
	b (J mol ⁻¹)	13.12	b (J mol ⁻¹)	78.92	b (J mol ⁻¹)	17.27
	R ²	0.8910	R ²	0.9071	R ²	0.9171

Table S6. Comparison of adsorption of MB by different adsorbents.

Adsorbent	Adsorption capacity (mg/g)	Ref.
MIL-121	303.00	2
ZnBDC	55.00	3
[BMIM][PF ₆]/MIL-53 (Al)	204.90	4
rht MOF	708.00	5
fibril-UiO-66-NH ₂ aerogels	25.20	6
NH ₂ -MIL-88(Fe)	591.72	7
UiO-66	370.00	8
(Ce)-UiO-66	110.00	9
amino-MIL-101 (Al)	762.00	10
UiO-66-NH ₂ @MCS	400.90	11
RAC-ADUF	238.48	12
IUAC	344.83	13
SS-derived carbon	964.63	14
HOF-NBDA	594.09	15
JZS-1	446.40	16
TpPa COF/CS	831.30	17
TzDABA COF	315.00	18
MF@COF	947.00	19
ZJU-64-Me	232.98	This work
ZJU-64-Me@SA	740.17	This work

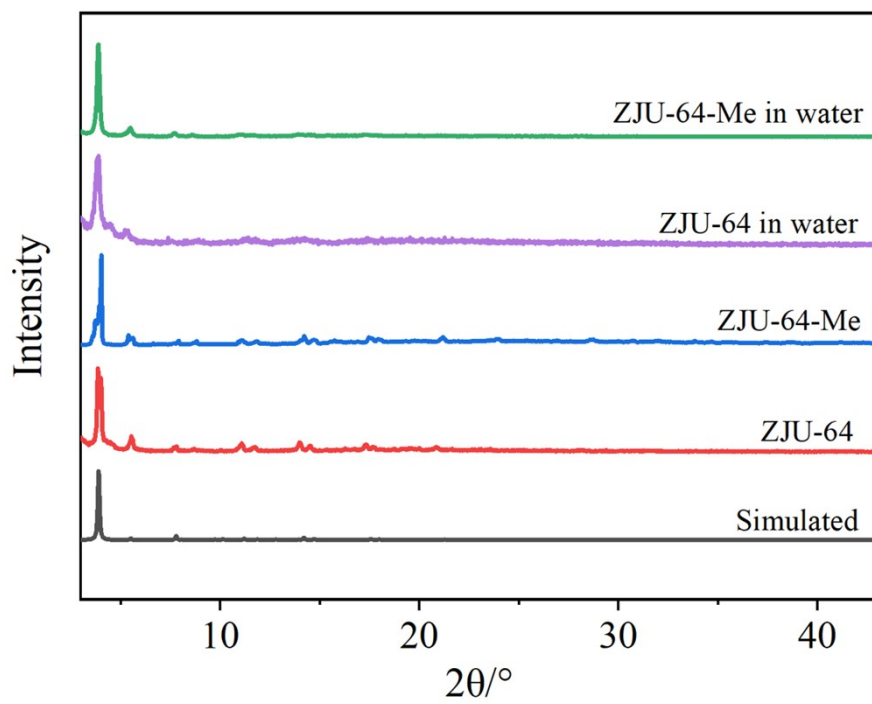


Fig. S1 PXRD patterns of ZJU-64 and ZJU-64-Me.

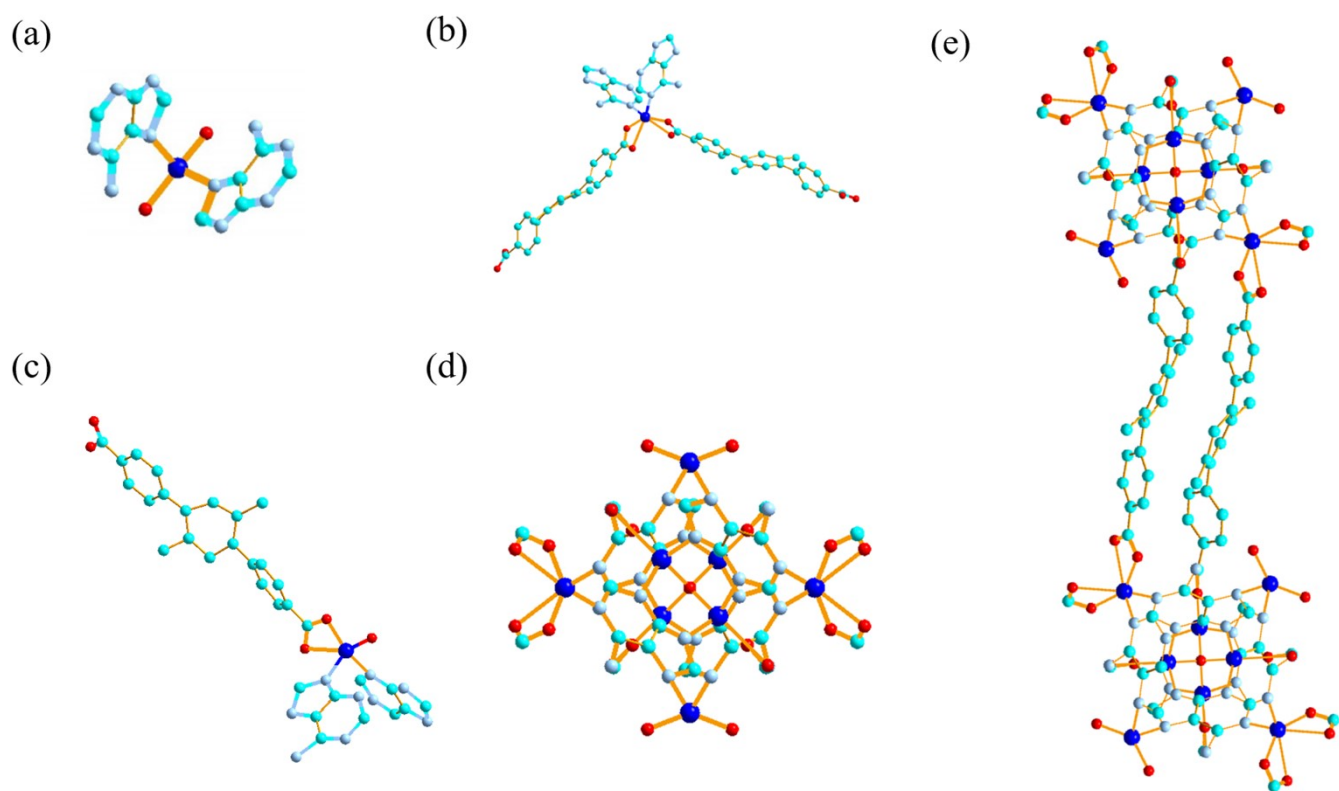


Fig. S2 The coordination mode of (a) Zn1, (b) Zn2 and (c) Zn3. (d) The Zn clusters of ZJU-64-Me viewed along the *c*-axis. (e) The connection mode of organic ligands and the Zn clusters. Blue, cyan, sky blue and red represent Zn, C, N, O. All H atoms are omitted for clarity.

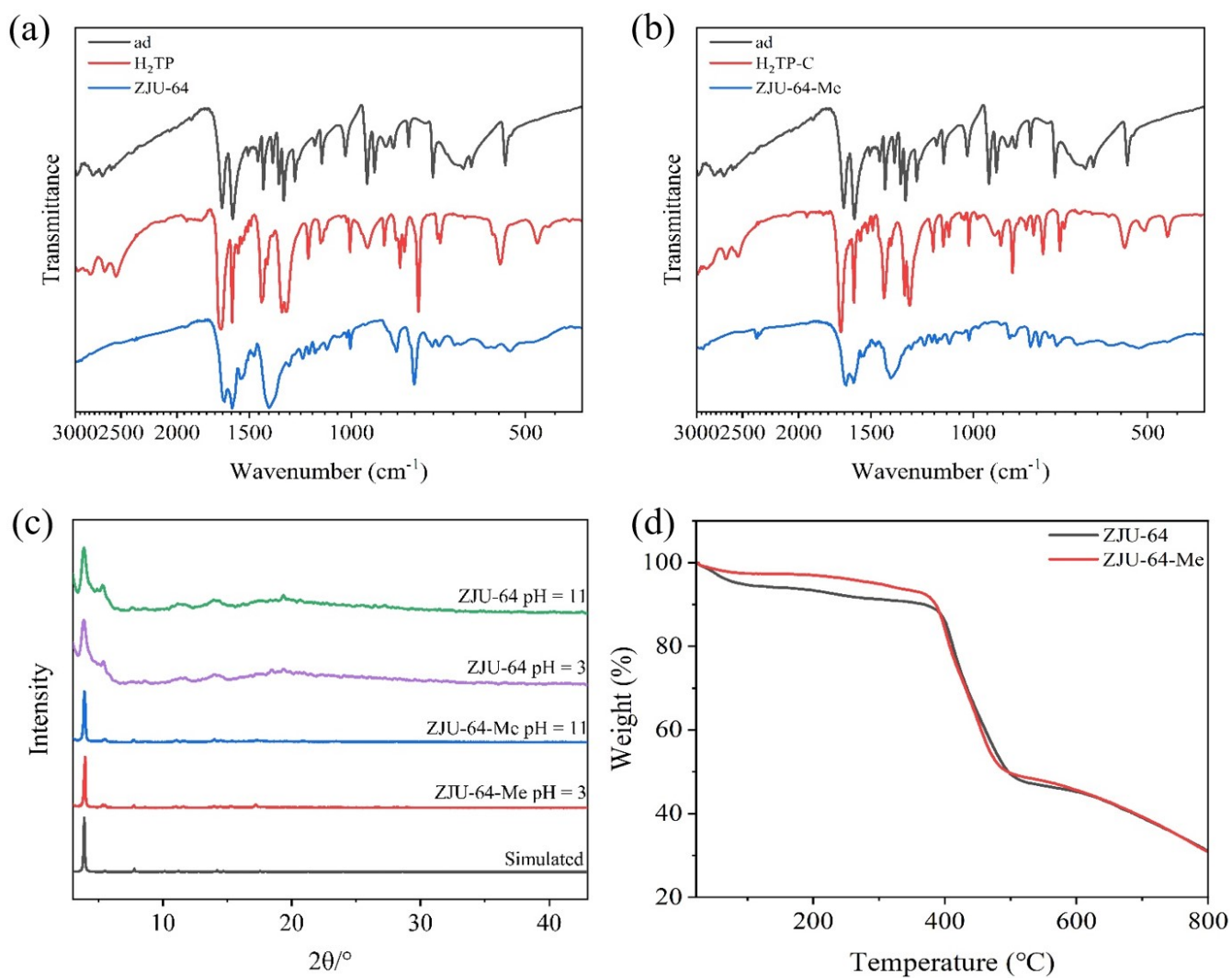


Fig. S3 (a) FTIR spectra of ligand ad, H₂TP and ZJU-64. (b) FTIR spectra of ligand ad, H₂TP and ZJU-64-Me. (c) PXRD patterns of ZJU-64 and ZJU-64-Me after immersion in solutions of pH=3 and pH=11. (d) TGA curves of ZJU-64 and ZJU-64-Me under nitrogen atmosphere.

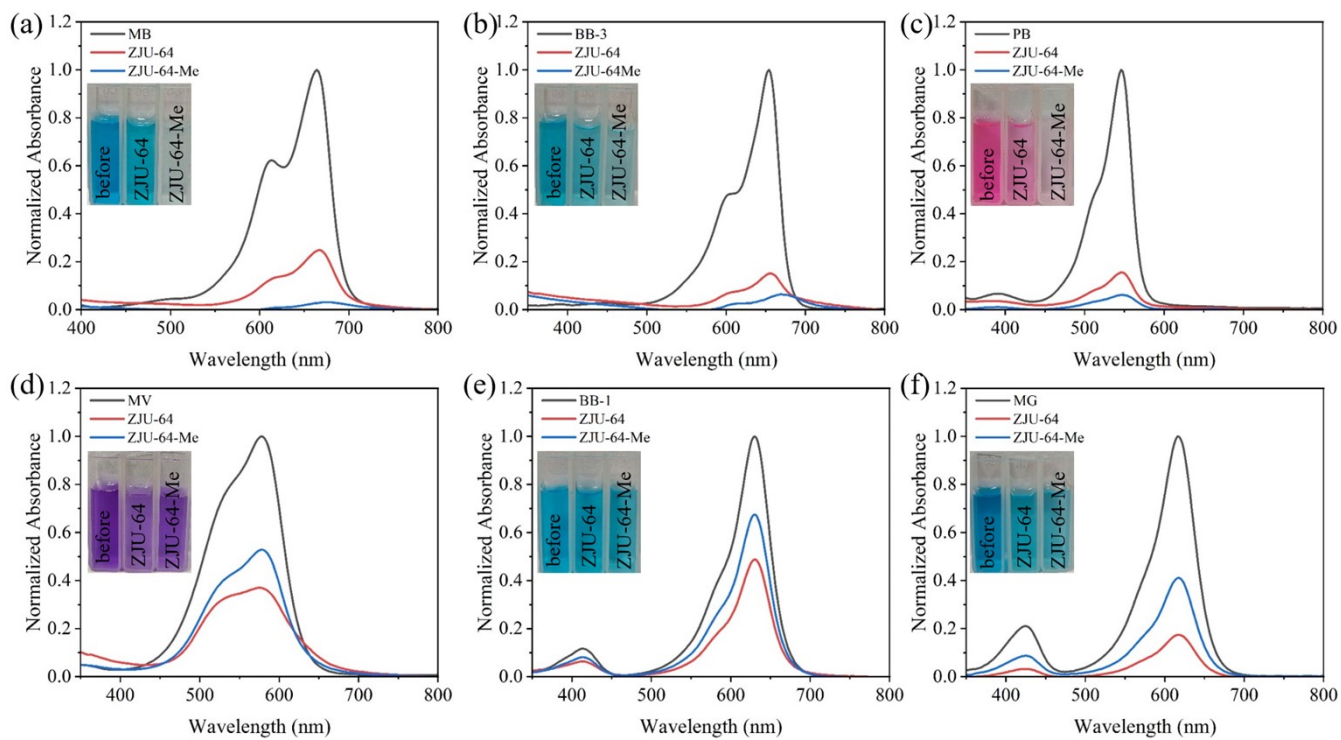


Fig. S4 Changes in the UV-vis adsorption spectra of cationic dyes (a) MB, (b) BB-3, (c) PB, (d) MV, (e) BB-1 and (f) MG after the addition of ZJU-64 and ZJU-64-Me.

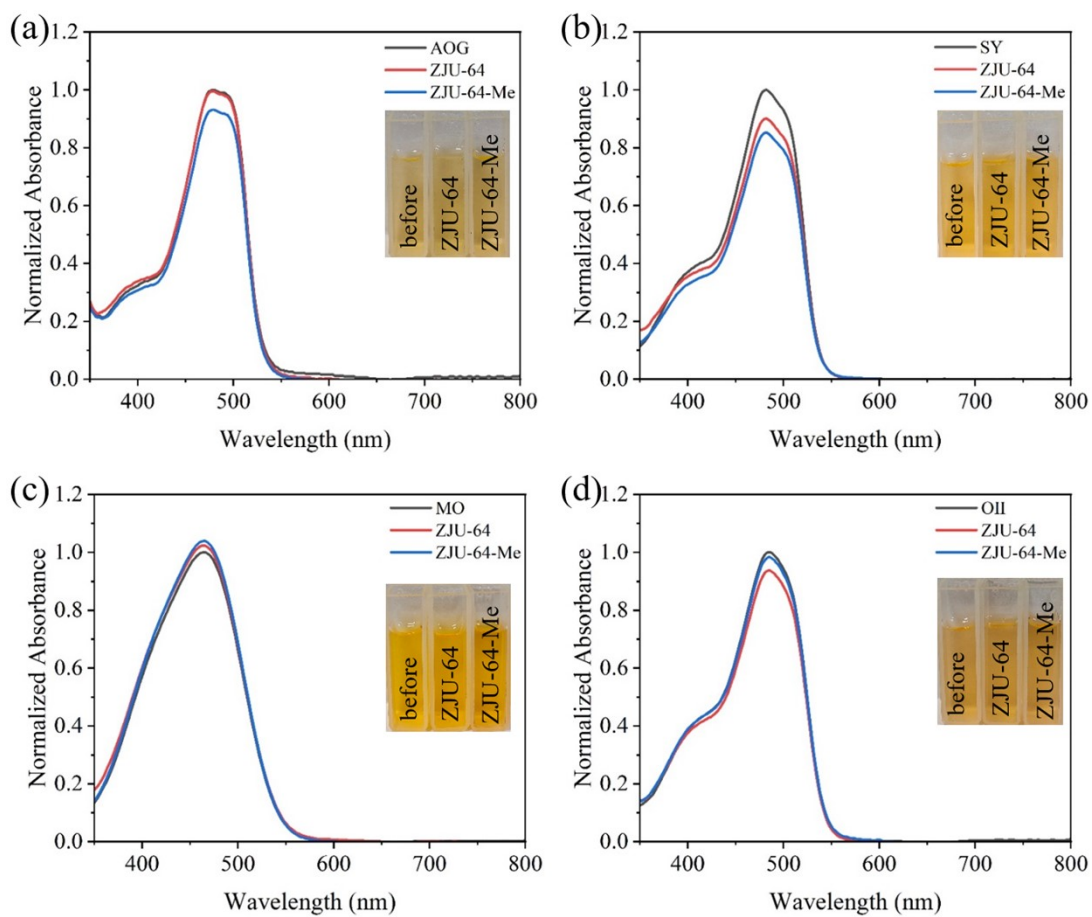
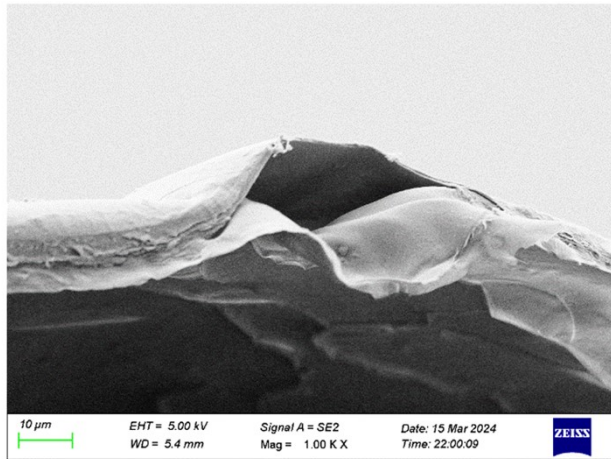


Fig. S5 Changes in the UV-vis adsorption spectra of anionic dyes (a) AOG, (b) SY, (c) MO, (d) OII after the addition of ZJU-64 and ZJU-64-Me.

(a)



(b)

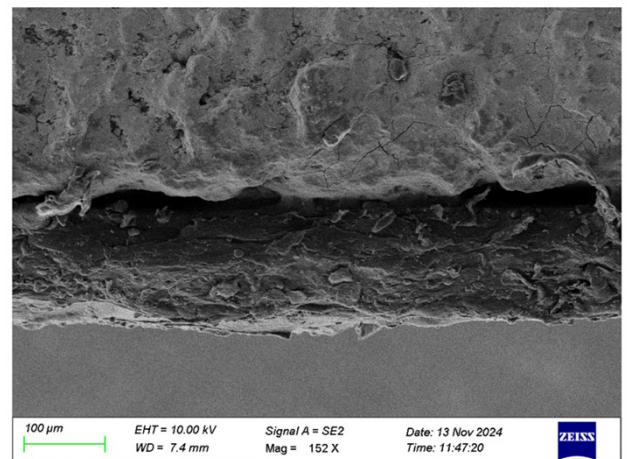


Fig. S6 SEM images of (a) SA, (b) ZJU-64-Me@SA.

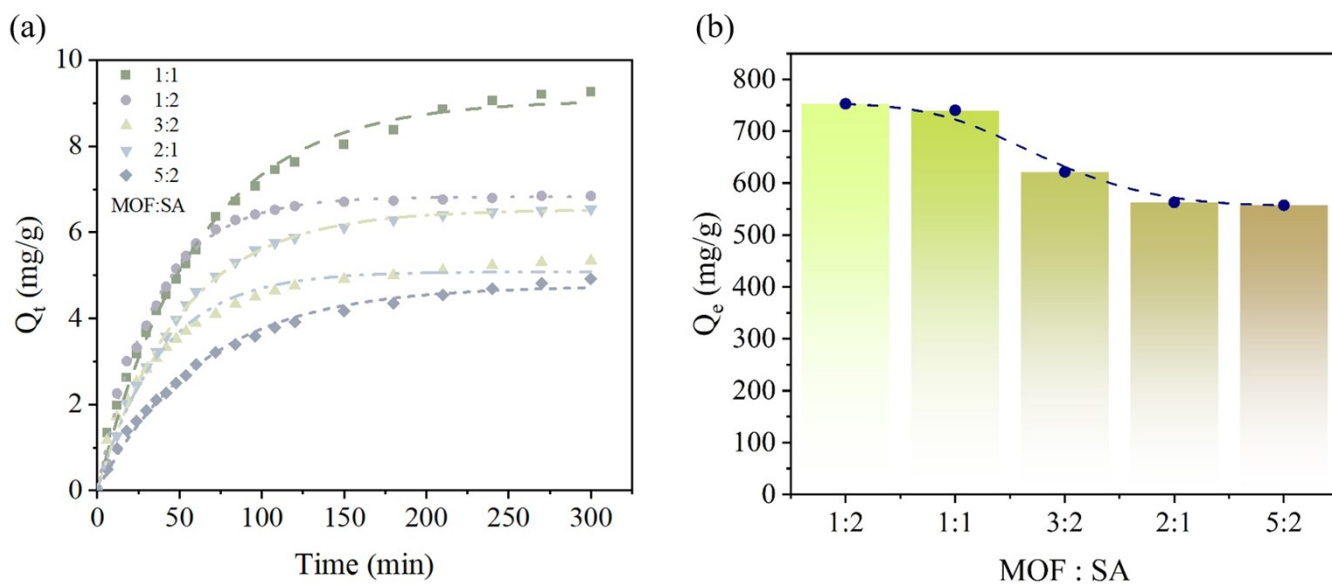


Fig. S7 (a) Kinetics and (b) maximum adsorption of MB with different ratios of ZJU-64-Me and SA.

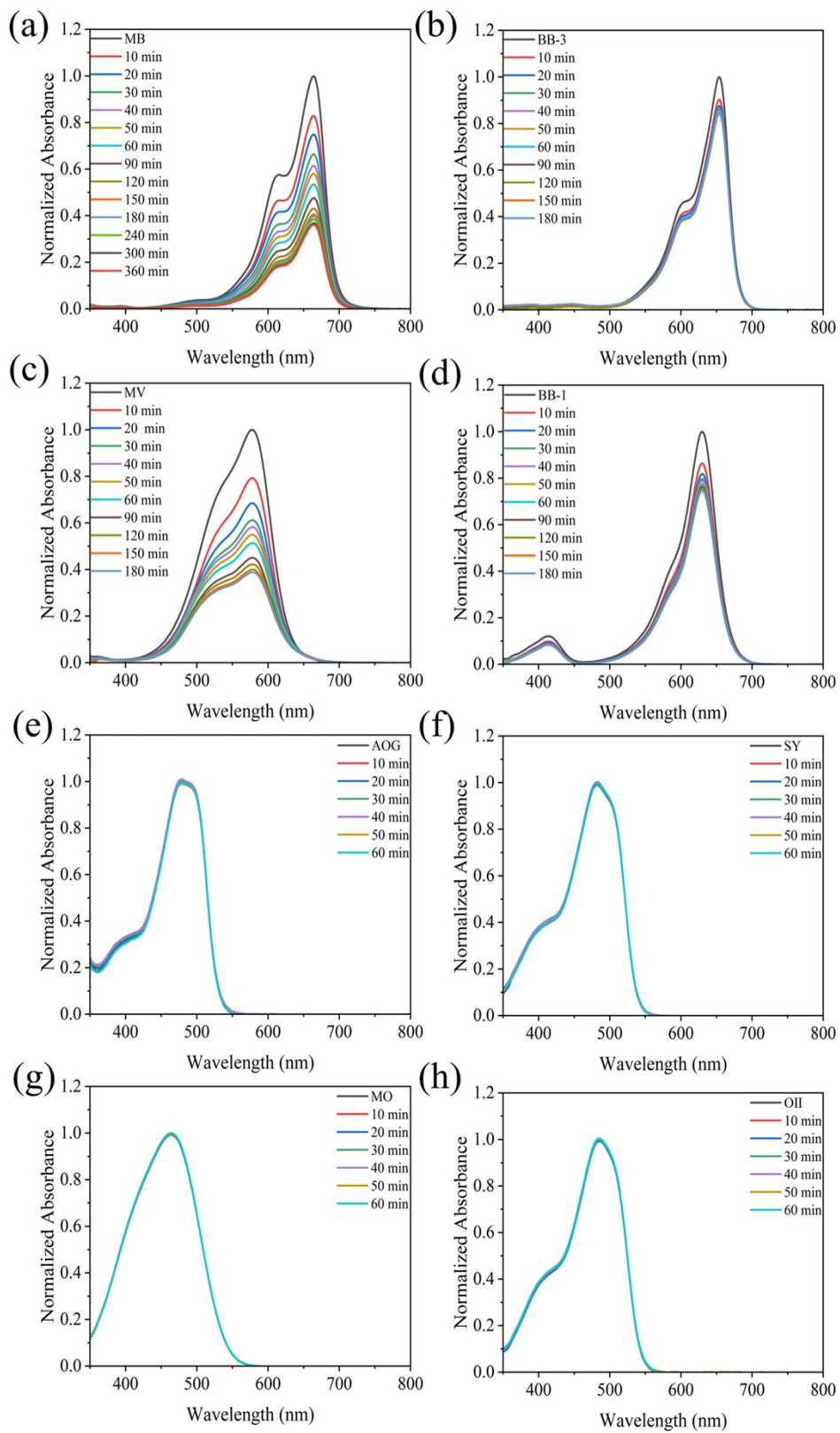


Fig. S8 Changes in the UV-vis adsorption spectra of (a) MB, (b) BB-3, (c) MV, (d) BB-1, (e) AOG, (f) SY, (g) MO, (h) OII after the addition of SA.

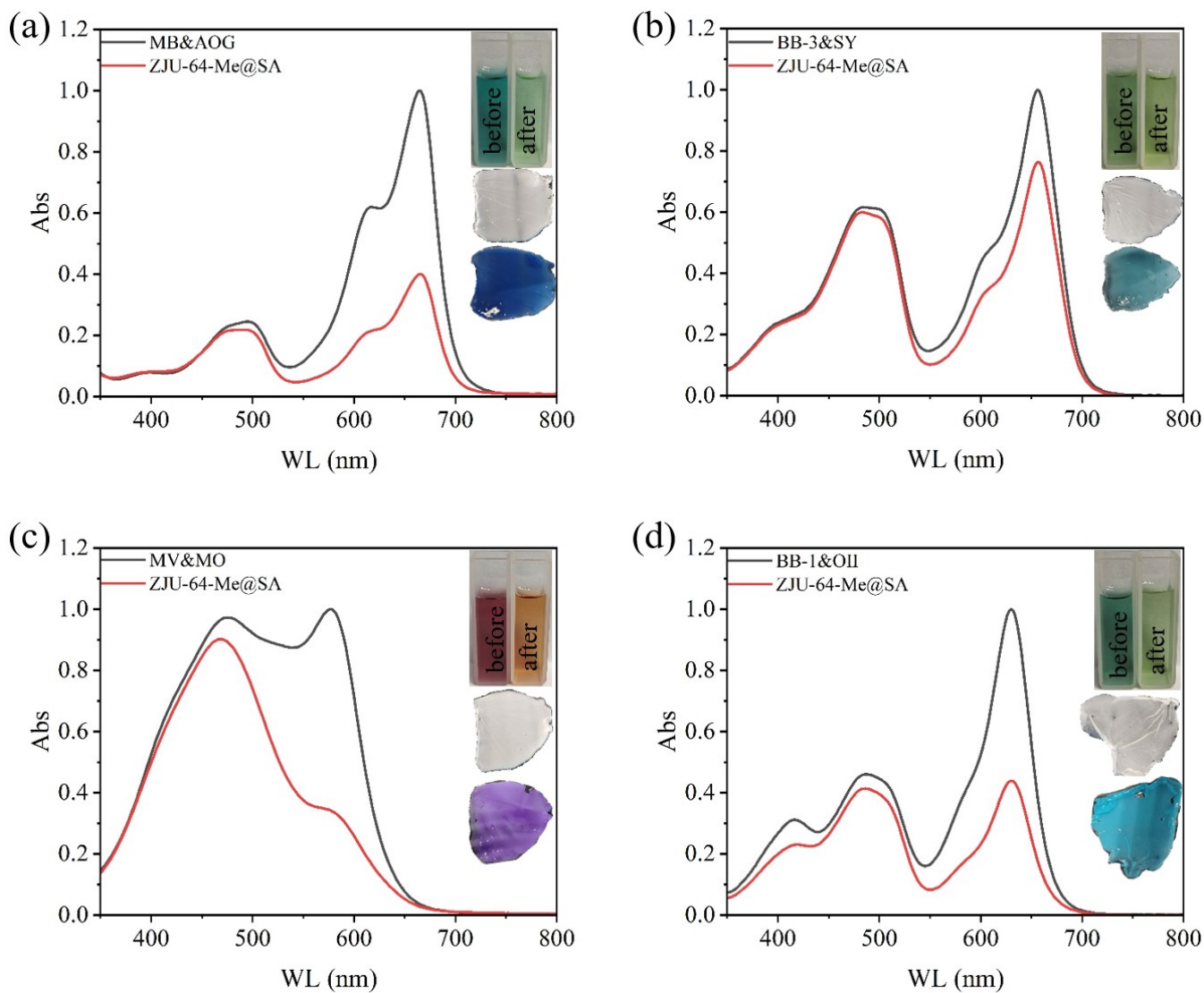


Fig. S9 Changes in the UV-vis adsorption spectra of mixtures of (a) MB&AOG, (b) BB-3&SY, (c) MV&MO and (d) BB-1&OII after the addition of ZJU-64-Me@SA.

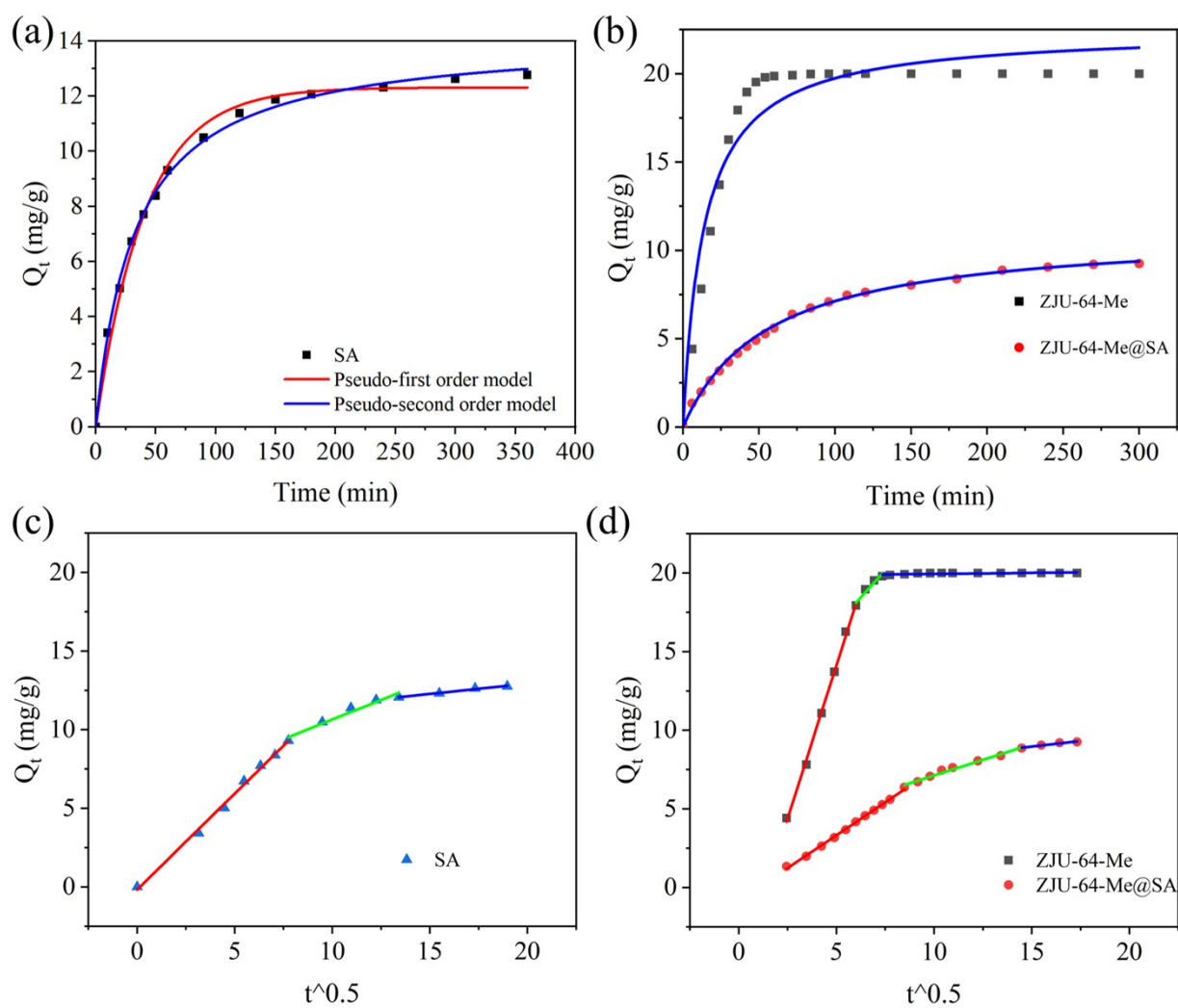


Fig. S10 (a) Kinetic Models of SA. (b) Pseudo-second-order model of ZJU-64-Me and ZJU-64-Me@SA. Internal diffusion model of (c) SA, (d) ZJU-64-Me and ZJU-64-Me@SA.

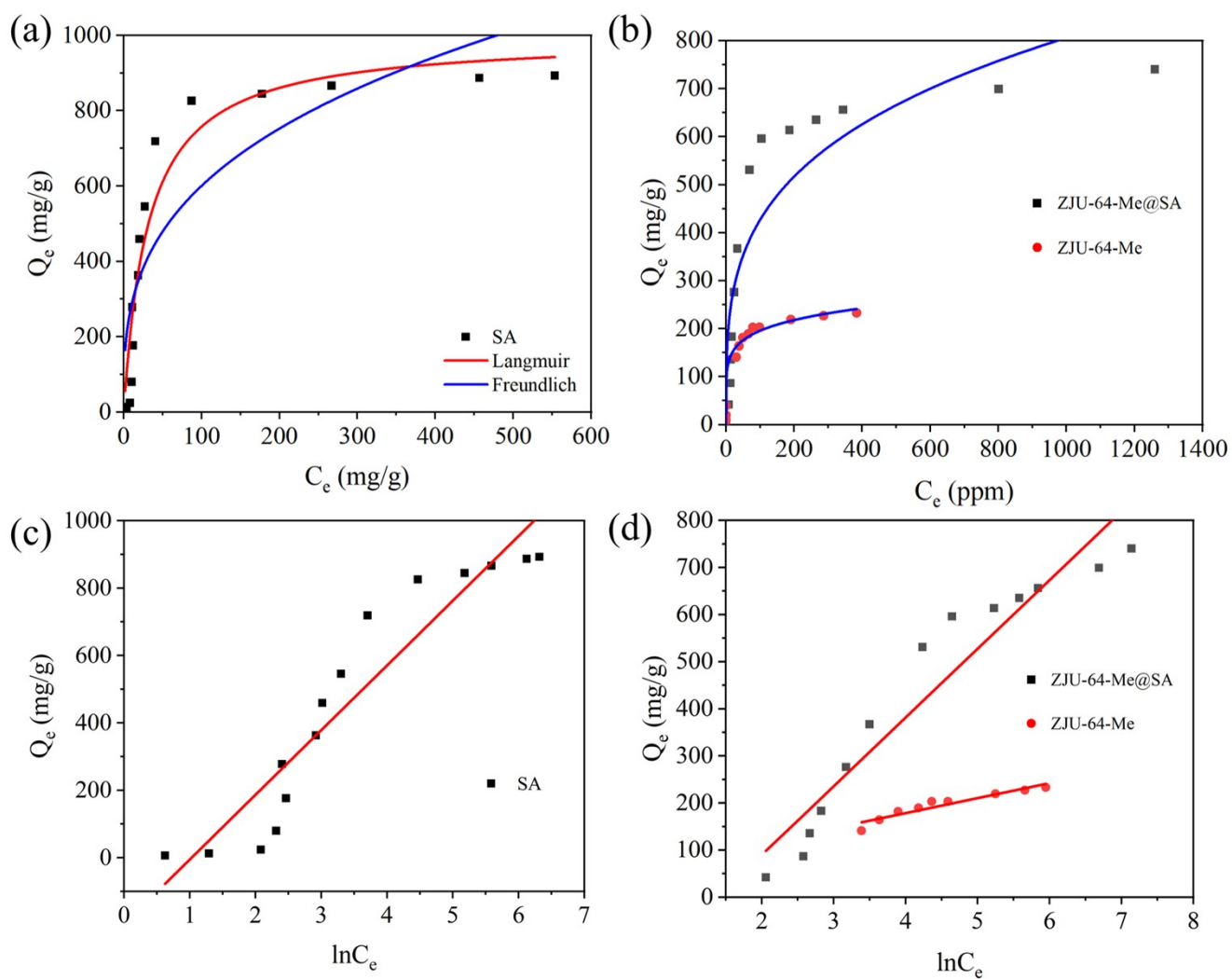


Fig. S11 (a) Isotherm Models of SA. (b) Freundlich model of ZJU-64-Me and ZJU-64-Me@SA. Temkin model of (c) SA, (d) ZJU-64-Me and ZJU-64-Me@SA.

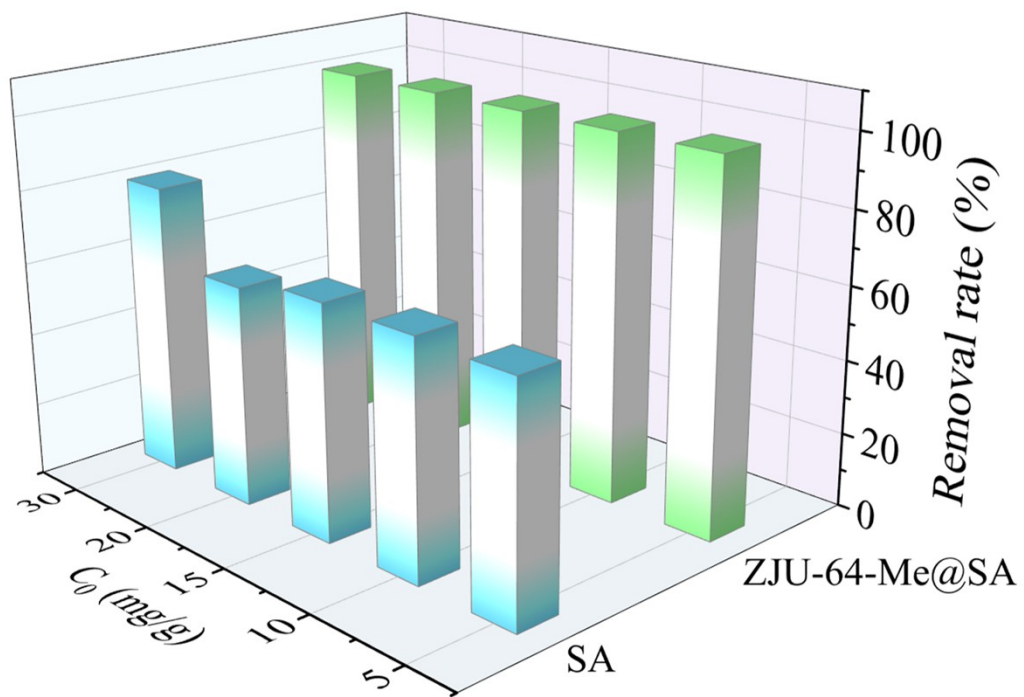


Fig. S12 MB removal rate at low concentrations of SA and ZJU-64-Me.

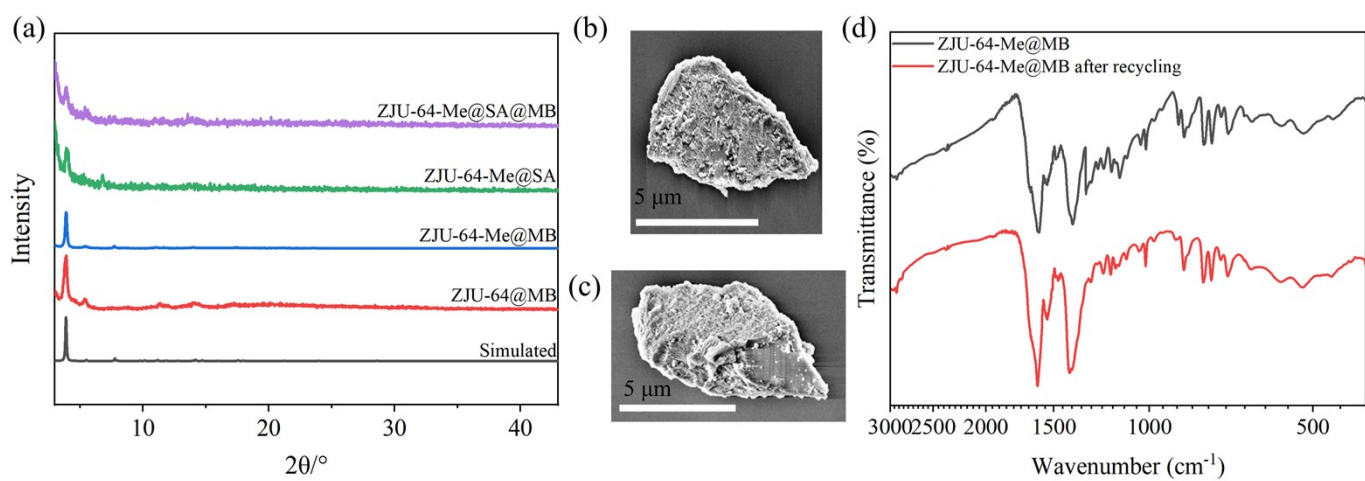


Fig. S13 (a) PXRD of ZJU-64@MB, ZJU-64-Me@MB, ZJU-64-Me@SA and ZJU-64-Me@SA@MB. SEM images of crystals (b) before and (c) after recycling. (d) FTIR patterns of crystal before and after recycling.

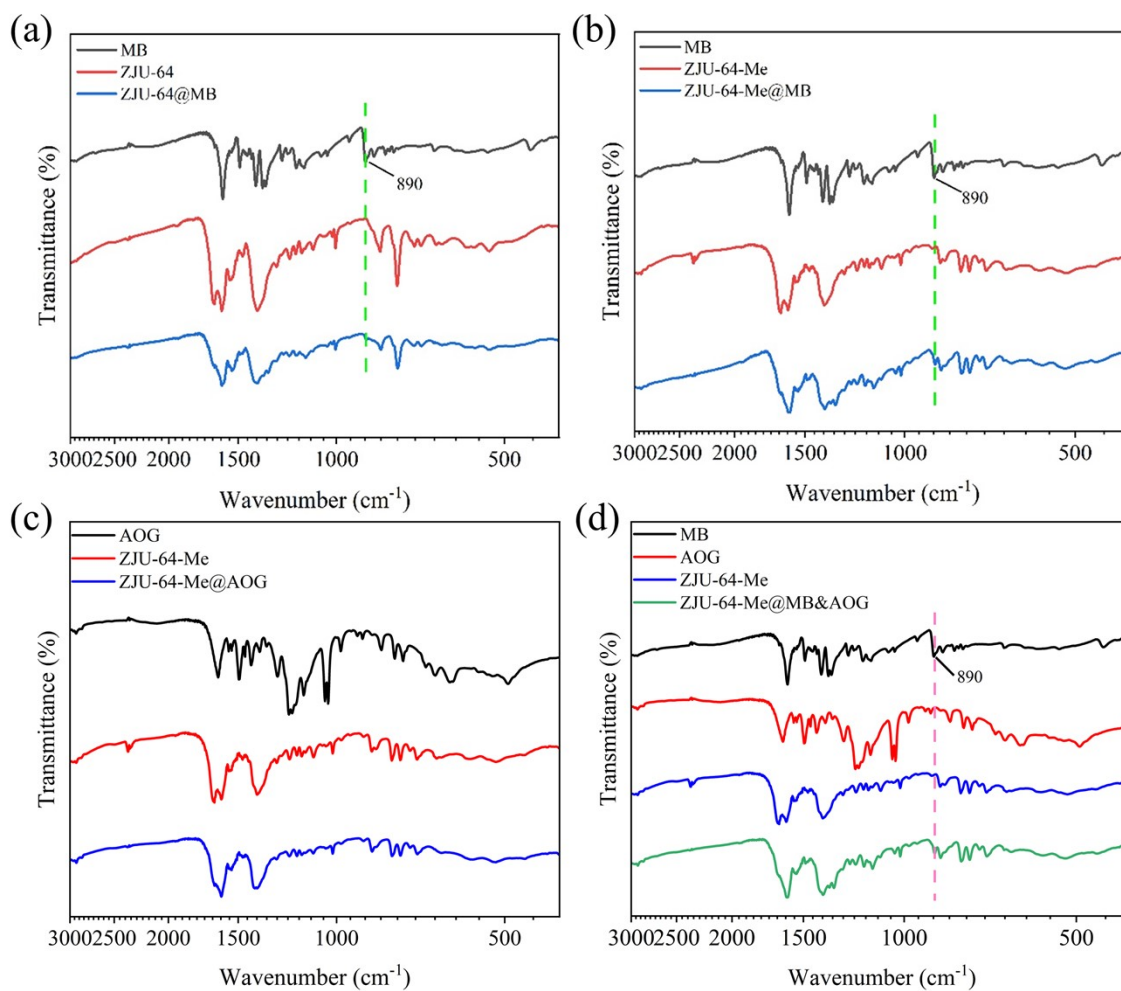


Fig. S14 FTIR spectra of (a) ZJU-64 and ZJU-64@MB, (b) ZJU-64-Me and ZJU-64-Me@MB, (c) ZJU-64-Me and ZJU-64-Me@AOG, (d) ZJU-64-Me and ZJU-64-Me@MB@AOG. The aromatic ring vibration peaks of MB were observed at 890 cm^{-1} in MOFs after the adsorption of MB. The characteristic peaks of AOG were not observed in MOFs after the adsorption of AOG and MB&AOG mixed dye.

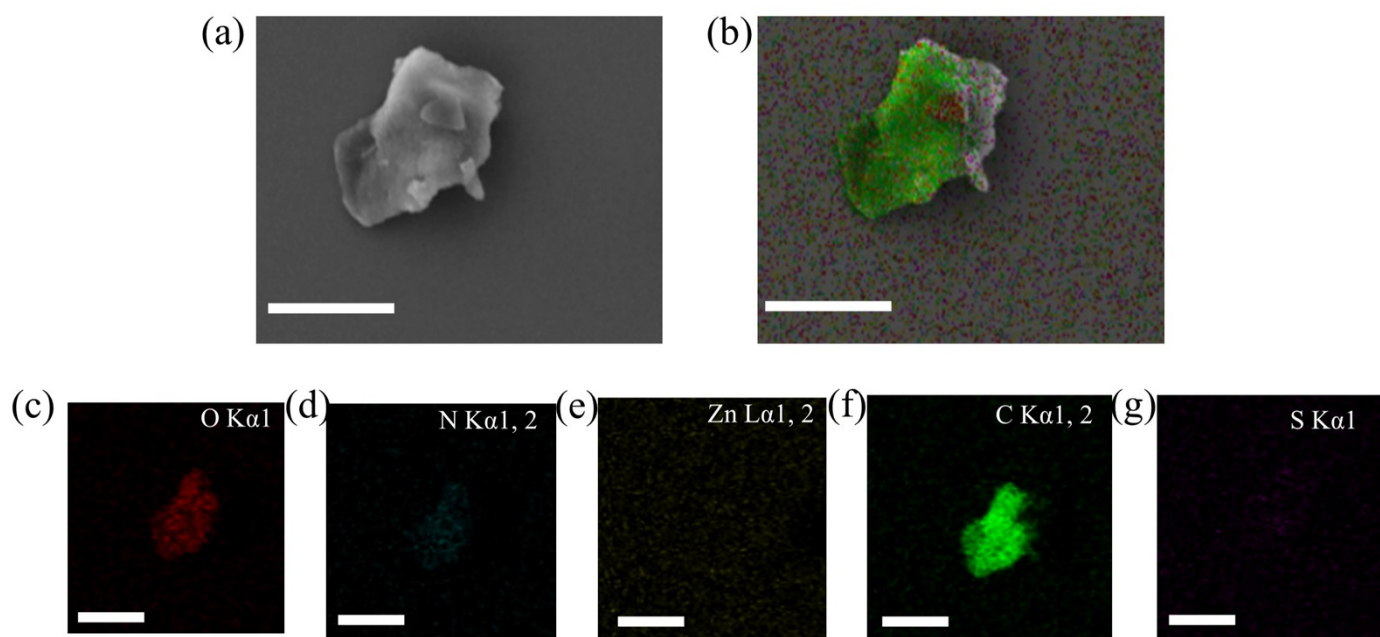


Fig. S15 (a) SEM images of ZJU-64-Me. (b) Merge image of ZJU-64-Me and (c-g) elemental mapping of O, N, Zn, C, and S. Scale bar, 20 μ m.

Reference

1. W. Lin, Q. Hu, J. Yu, K. Jiang, Y. Yang, S. Xiang, Y. Cui, Y. Yang, Z. Wang and G. Qian, *ChemPlusChem*, 2016, **81**, 804-810.
2. N. Hu, F. Hang, K. Li, T. Liao, D. Rackemann, Z. Zhang, C. Shi and C. Xie, *Sep. Purif. Technol.*, 2023, **314**, 123650.
3. E. B. AttahDaniel, F. M. Mtunzi, D. Wankasi, N. Ayawei, E. D. Dikio and P. N. Diagboya, *WATER AIR SOIL POLL.*, 2022, **233**, 10.1007/s11270-11022-05912-11272.
4. S. Kavak, Ö. Durak, H. Kulak, H. M. Polat, S. Keskin and A. Uzun, *Front. Chem.*, 2021, **8**, 10.3389/fchem.2020.622567.
5. Z. Zhu, Y.-L. Bai, L. Zhang, D. Sun, J. Fang and S. Zhu, *Chem. Commun.*, 2014, **50**, 14674-14677.
6. M. Peydayesh, X. Chen, J. Vogt, F. Donat, C. R. Müller and R. Mezzenga, *Chem. Commun.*, 2022, **58**, 5104-5107.
7. N. Hassan, A. Shahat, I. M. El-Deen, M. A. M. El-Afify and M. A. El-Bindary, *J. Mol. Struct.*, 2022, **1258**, 132662.
8. F. Ahmadjokani, R. Mohammadkhani, S. Ahmadipouya, A. Shokrgozar, M. Rezakazemi, H. Molavi, T. M. Aminabhavi and M. Arjmand, *Chem. Eng. J.*, 2020, **399**, 125346.
9. R. M. Rego, G. Sriram, K. V. Ajeya, H.-Y. Jung, M. D. Kurkuri and M. Kigga, *J. Hazard. Mater.*, 2021, **416**, 125941.
10. E. Haque, V. Lo, A. I. Minett, A. T. Harris and T. L. Church, *J. Mater. Chem. A*, 2014, **2**, 193-203.
11. Y. Yang, Y. Guo, Z. Qiu, W. Gong, Y. Wang, Y. Xie and Z. Xiao, *Carbohydr. Polym.*, 2024, **328**, 121750.
12. Z. Li, X. Luo and Y. Li, *ACS Omega*, 2022, **7**, 43829-43838.
13. A. El Nemr, A. G. M. Shoaib, A. El Sikaily, A. E.-D. A. Mohamed and A. F. Hassan, *Environmental Processes*, 2021, **8**, 311-332.
14. S. Li, M. Li and X. Zhang, *Macromol. Res*, 2024, **32**, 443-452.
15. R. Zhu, Q. Wu, S. Lin, L. Wang, Y. Liang, L. Zhang, D. Zhao, Y. He and B. Chen, *Chem. Commun.*, 2024, **60**, 14660-14663.
16. Y.-J. Hou, S. Fang, X.-Y. Zhang, J. Wang, Q. Ruan, Z. Xiang, Z. Wang and X.-J. Zhu, *ACS Appl. Mater. Interfaces.*, 2022, **14**, 49875-49885.
17. Z. Ji, M. Li, X. Li, E. Jin and W. Linghu, *Fibers Polym.*, 2023, **24**, 2039-2053.
18. R. Li, K. Zhang, X. Yang, R. Xiao, Y. Xie, X. Tang, G. Miao, J. Fan, W. Zhang, S. Zheng and S. Cai, *Sep. Purif. Technol.*, 2024, **340**.
19. Y. Zhu, Y. Liu, S. Xue, H. Yang, X. Han, C. Zhang, G. Duan, Y. Huang, H. Mao, C. Ma and S. Jiang, *Int. J. Biol. Macromol.*, 2025, **313**.